Teknik Dergi, 2022 12501-12524, Paper 692

Investigating the Influence of Dam-Breach Parameters on Dam-Break Connected Flood Hydrograph

Mohamed NAJAR[1]
Ali GÜL[2]

ABSTRACT

The dam-break connected flood hydrograph properties primarily depend on the breach geometry and the time for the breach to fully develop. Therefore, the prediction of dam's breach geometry is essential in dam-break studies. To understand the impact of breach parameters on flood peak hydrograph, five of the most common breach prediction methods are implemented in the presented study to estimate the flood hydrographs using 2-dimensional HEC-RAS model. The Ürkmez Dam is chosen as the case study due to the presence of a residential settlement located right at the dam downstream where undesirably any breach of the dam body can have inevitable and dramatical risks on downstream populations and properties. Various levels for reservoir storage are investigated in each method. To assess the impact of each breach parameter on the resulting flood hydrographs, sensitivity analysis is carried out. The peak discharge rates and the times to peak for each analyzed scenario are investigated and discussed. Results reveal that Froehlich approach is the most reasonable method for estimating dam-breach parameters as far as exemplified in the Ürkmez Dam case. Furthermore, sensitivity analysis points out that the parameter of the breach side slope has no major influence on the time to peak while having an insignificant impact on the peak discharge. Besides, the study exhibits that both the peak discharge and the time to peak characteristics are highly sensitive to breach time formation parameter. In the light of these targeted findings, the study is aimed to contribute to other relevant research in designating the set of key parameters in experimental or modeling efforts in a way to limit the uncertainty that substantially originates from personal judgment.

Keywords: Dam-break, dam breach flows, sensitivity analysis, uncertainty, flood hydrograph, Ürkmez Dam.

Note:
- This paper was received on September 17, 2020 and accepted for publication by the Editorial Board on March 10, 2021.
- Discussions on this paper will be accepted by November 30, 2022.

• https://doi.org/10.18400/tekderg.796334

1 Dokuz Eylül University, Graduate School of Natural and Applied Sciences, GIS Dept., Izmir, Turkey
eng.mhmd.najar@gmail.com - https://orcid.org/0000-0002-9107-961X

2 Dokuz Eylül University, Department of Civil Engineering, Izmir, Turkey
ali.gul@deu.edu.tr - https://orcid.org/0000-0001-8137-8950

1. INTRODUCTION

Dams are hydraulic structures that regulate the flow of rivers. They primarily serve to collect and control the water stored in their reservoirs for several purposes (e.g., hydropower generation, water supply, irrigation, etc.). Even though dams afford great benefits to societies, they could cause catastrophic damages for lives, properties, and environment in cases of accidental events or other emergency conditions. Dam-break (widely also called dam-breach) is a term used when the water behind the dam is released accidentally. Dam-break takes place due to various reasons (e.g., structural defects, insufficient spillway capacity, seepage & piping, overtopping, earthquakes, etc.).

When designing the dams, the failure probability is assigned to be very low during their operational life span. Dam critical design principles demand the dams to resist different kinds of loads, specifically dam body weight and storage water load in the upstream reservoir, with or without seismic load. The failure of a water retaining structure can be categorized with respect to the level of failure (e.g., partial or complete) or its duration (e.g., sudden or gradual). Sudden failure is associated with all types of dams: concrete dams, embankment or arch dams. When breaching is initiated; its development is faster for earth-fill dams than other types under the same conditions. Rock-fill and earth-fill dams - referred to as embankment dams, constitute the most significant portion of dams around the world. Thus, most events of dam-break are recorded for this category. Their failure, depending on the triggering factors, is mostly a gradual process rather than a sudden one.

Different factors can initiate the failure of the earth-fill dam, e.g., piping, overtopping, seepage, or foundation defect. One of the most basic failure modes for embankment dams is the overtopping. Overtopping failure occurs when the inflows become higher than the design inflow [1], malfunctioning reasons, lack of spillway operation systems, inadequate capacity of spillways, or as a consequence of landslides into the reservoir. Any earth-fill dam would collapse if the spillway capacity were inadequate and flood wave elevates high enough to stream over the crest of the dam for a fair amount of time; the initial breach would then start. Once the initial breach mechanism begins, and the upstream storage water levels continue to be high, the breaching would persist in developing and any effort made to stop it would be ineffective [2]. Overtopping failure mode may not lead to structural collapse, but still presents a significant flood hazard. Similarly, the rapid release of upstream stored water to drop the water level to safe limits could conclude to not commendable consequences for downstream areas [3]. The penetration of the water through the interior body of the dam or its foundation may progressively weaken soil from the embankment or its foundation, leading to the failure of the dam. Here, piping failure mode can be defined as a failure caused by water seeping through the dam's body, bearing with its small particles of dam material, continuously enlarging the gap [1].

In the recent decade, several researchers extensively studied both the dam breaks and the flood-wave propagation in both one-dimensional and two-dimensional models. Li et al. [4] examined six reservoirs - located north of Italy, to evaluate the flood damages to the downstream regions. The HCH/DIGHE model was used to measure the hydrograph generated from a dam-break flood event in a way combined with MIKE11 (1D) model to simulate the flood-wave in the downstream riverbed. The study covered also, some issue connected to dam-breach, the impact of the dam-breach parameters, and calculation of the

hydraulic resistance factors. Two early studies by Bozkuş and Kasap [5] and by Bozkuş and Güner [6] employed numerical models for simulating dam break flood events. Based on the comparison of the findings of these studies and an experimental physical dam break model revealed that there is a substantial difference between the physical and numerical results implying that the time to peak discharge (T_p) is sensitive to the channel's bottom surface friction. Brufau et al. [7] modelled the flood wave propagation in both one and two dimensions using the shallow water flow equations for unsteady flow. Their model attempted to override the issue that arises when flow develops over dry beds of different slopes. Their model showed a satisfying performance in handling complex flow domains. Yanmaz and Beşer [8] investigated the safety of gravity dams by employing a probabilistic evaluation approach. A probabilistic strategy through random loading and resistance aspects were used for the safety analysis. One of the earliest two-dimensional models in the field of dam-breaks performed by Vásquez and Leal [9]. A finite element method was employed to discretize the computational domain by using a triangular mesh. Both dry (zero) and wet (non-zero) initial water depths were adopted as downstream boundary conditions to run the model. The model successfully simulated both the hydraulic jump that was produced from a wet downstream condition and the surge that was moving over an initially dry bed. Alcrudo and Mulet [10] studied the Tous Dam, which was experienced with a major dam-break event in 1982, to develop and validate a flood wave model. Due to the absence of a validated topography model of the area prior to dam-break occurring time, they run the flood propagation model on two different topography estimates to understand the uncertainties associated with the terrain variety. Palumbo et al. [11] simulated the dam-break flow by taking into consideration the turbulent stresses that may appear from the re-circulating flows in a limited extent. Macchione [12] developed a model to present the main aspects influencing both the formation of the hydrograph peak discharge and the breach development. He described the breach occurrence as a function of the shear stress generated by the flow. The geometry of the embankment, the shape of the breach and the planimetric shape of the reservoir had been taken into consideration. The result after the model calibration indicated a high accuracy of the physical layout for both overtopping and piping failure modes. In the following study by Macchione and Rino [13], sensitivity analysis was carried out to quantify the influence of the side slope parameter on the outputs. The sensitivity analysis showed that dam height, reservoir volume, and water mass in the reservoir are significant factors that influence the flood hydrograph. In a different effort that expands assessments through statistical analyses toward the estimation of expected breach parameters relationships, Froehlich [14] used the data compiled from 74 embankment dam failure cases and developed a set of empirical models for breach cases that form in the shape of a trapezoid. Based on the findings of the study, which also employed Monte Carlo simulation techniques to estimate the uncertainty degree of the predicted peak flows and water depths in the downstream, it was concluded that breach geometry has a non-vertical trapezoidal shape. Yochum et. al. [15], on the other hand, modelled an actual dam break event using the HEC-RAS model. Because the study adapted the actual breach geometry parameters, the obtained results have a good agreement with the depths collected as post-flood dataset. Ying et al. [16] developed a dam-break model based on the finite volume method using an unstructured triangular mesh. To simplify the computation and reduce the numerical imbalance between source and flux terms, the model considered the effects of pressure and gravity in the shallow water equations. The developed model displayed capacity to simulate dam-break connected flows which may take place over complicated terrains with different flow types (e.g., subcritical flows, supercritical flows, or

trans-critical flows). Singh et al. [17] developed a two-dimensional numerical model for simulation of dam-break flow propagation. Experiment with a frictionless horizontal bottom was established to validate the 2D model. The agreement observed between the simulation and the experimental results indicated that the model was suitable for simulating dam-break flows. Marco et al. [18] studied the failure of Gleno Dam - located in the Central Italian Alps, caused by structural deficiencies. The study attempts to set-up a dam-break model valid for a mountainous terrains. One-dimensional modelling of dam wave propagation with a first-order finite volume numerical scheme was used to present the main results of the study. Bozkuş and Bağ [19] simulated a fictitious dam break that takes place under a set of pre-defined conditions. Their analysis focused on the post-failure consequences and attempted to estimate the inundation depth with respect to time in the downstream valley. FLDWAV software was used to forecast the flood characteristic. Based on the outputs, a set of recommendations were suggested to the local administrators in charge of public safety. Honghai and Altinakar [20] integrated the GIS and remote sensing technologies to develop a decision support system for dam-break flood management formed on two-dimensional flood simulations. They used HEC-RAS & HEC-FDA to validate their system. The results indicate that the decision support system provides a reliable setting for estimating different flood damage. Mahdizadeh et al. [21] followed up on their previously introduced one-dimensional (1D) shallow-water model for simulating free-surface interaction with the flows issuing vertically through finite gaps. They enhanced the model by using a modified wave propagation algorithm (e.g., extends the shallow-water scheme to two dimensions) to understand the interaction between the free-surface flow and large underground pipe networks used for sewage and storm drainage. Navier-Stokes equations were employed to validate the algorithm. Bosa and Petti [22] applied a two-dimensional numerical model (e.g., 2DH model) to understand the impacts of the overtopping flood wave in the Piave Valley - a region in Italy witnessed a catastrophic dam-break in 1900; about 1700 individual passed away in the valley region alone. They verified if the simplifications assumed by the two-dimensional model properly simulated the growth of the wave. Tsakiris and Spiliotis [23] employed a semi-analytical approach to simulate the breach formation as well as to estimate the outflow hydrograph resulting from a hypothetical overtopping type dam break event. Assumptions of constant vertical erosion rate for the breach formation and a parabolic shape of the breach were accepted through the analysis. The study presented two sets of solution based on the capacity of the reservoir (e.g., prismatic or a power function of the water depth in the reservoir). Moramarco et al. [24] aimed to exemplify the collected reservoir levels data of the studied dam break event (i.e., partial sudden collapse of the spillway of the Montedoglio dam in December 2010) by using discharge hydrographs at several downstream river sites. The work employed a one-dimensional model to simulate the breach development and the flood wave propagation in the downstream valley. In this study, the breach development time was obtained by using an optimization method. Several modeling studies were conducted to scrutinize the effect of densely populated areas subject to the propagation of dam break generated flood waves. For the models using coarse grid sizes, Chen et al., [25] employed two parameters, building coverage ratio (BCR) and conveyance reduction factor (CRF), to simulate flooding in an urban region by two-dimensional model. They found out that this enhanced the accuracy of the modeling and slightly increased the computational efficiency. In addition, Chen et al., [26] utilized a multi-layer approach to model dam break flood plain by taking into considerations two additional factors, elevation and roughness, over those of their previous study. The multilayer approach further increased the accuracy of

the model at grid cells around the buildings and marginally facilitated the computation. Bellos and Tsakiris [27] simulated a flood event in a built-up area using a fully dynamic numerical model (FLOW-R2D). They solved the two-dimensional Shallow Water Equations using the Finite Difference Method and the McCormack numerical system. The resistance caused by buildings (e.g., the reflection boundary, the local elevation rise, and the local increase of the Manning roughness coefficient) were employed to examine the performance of the model. The study concluded that the reflection boundary method proved to be the foremost successful building representation when applying FLOW-R2D model. Elçi et al., [28] investigated the impact of buildings and other obstacles defined through using two parameters, Area Reduction Factor (ARF) and Width Reduction Factor (WRF), on the propagation of the flood waves from dam break events in the examples of two separate dams by combining one-dimensional HEC-RAS and two-dimensional FLO-2D models. They assessed the associated impacts on flood velocity and depth by comparing three scenarios ranked with varying breach characteristics [29].

The literature mainly focused on the determination of flow characteristics at the break time, the collapse mechanism and flood-wave propagation, using both numerical idealized and experimental models. The presented research employs the case-study of Ürkmez Dam to examine failure consequences of any break event that may occur in the site under certain triggering conditions, counting on the significance of the populated downstream region which is greatly used for vacation houses and touristic purposes. In case of a flood resulting from a dam-break event, the loss of lives and properties would be disastrous. In this context, a number of previous studies were carried out to simulate the flood-wave in the downstream area of the dam. Güney et al. [30] carried out an experimental model to simulate the flood-wave propagation by construction a distorted physical model of Ürkmez Dam with vertical and horizontal scales of 1/30 and 1/150, respectively. The model consists of an upstream reservoir, dam body, and topographical representation of downstream region. As the model represents the topography and the building in the downstream area, the effect of the agriculture existence on the flood wave was not covered. Haltas et al. [31] utilized the one-dimensional hydraulic routing HEC-RAS model to estimate the flood hydrograph generated from a partial failure of the dam. Then, a two-dimensional routing model FLOW-2D was employed to simulate the spreading of the dam-break flood after the flood wave exits the valley. A very recent study - following the work of Güney et al. [30]– was carried out by Oguzhan and Aksoy [32]. The study aimed to understand the vegetation effects on the flood wave propagation resulting from a dam-break. It was shown that the presence of vegetation makes a significant decrease in water depths as the flood wave propagates and considerably reduces flooding impact on the downstream settlements.

The previous research show that dam-break studies have two central tasks: estimating the breach flood hydrograph and routing the generated hydrograph along the narrow valley downstream of the dam site. However, the flood hydrograph is determined by the breach geometry and breach formation time. In the dam break simulation models the user is required to estimate the breach geometry and dimensions independently and provide this information as input to the simulation model. Therefore, breach geometry prediction depends on personal judgments, thus it involves high uncertainty in estimating dam-break flood. To this end, the objectives of this study are: (1) to examine the impact of dam-break parameters on maximum breaching outflows, (2) to evaluate the effect of each breaching parameter on the resulting

flood hydrographs by carrying out a sensitivity analysis, and (3) to generate spatio-temporal series of hazard maps to be observed during the propagation of the flood waves to occur from varying approaches of dam break prediction, eventually to help decision makers, and vulnerable communities in the final end, against the flooding threat and for the sake of emergency preparedness. Concerning the targeted objectives in a way this study differs from the previous studies, in terms of (1) the consideration of five modelling approaches against comparatively different selections of some previous studies toward assessing dam break parameters, (2) the use of method-specific breach parameter estimations instead of user defined parameter assignments, (3) the consideration of Probable Maximum Flood (PMF) based on the computation of Probable Maximum Precipitation (PMP) to represent the worst-case scenario in hydrologic aspect, (4) the topography mapping based on precise and updated Digital Terrain Model (DTM) that represents the dam site downstream accurately by adapting the building volumes and other cadastral features onto the Digital Elevation Model (DEM) as well as the accurate reservoir geometry definition to allow level pool routing, (5) final disposition of hazard map series to aid in decision-making.

2. DAM BREAK PHENOMENON

2.1. Dam Breach Characteristics

Dam breaching is a very complex, time-dependent and non–linear mechanism. With the aim of avoiding non-linearity of the model, a simplification might be made regarding breach shape. Breach shape is usually predefined in the models. A uniform erosion behavior during the breaching development time and a constant breach shape are assumed. The breach cross-section is usually considered to be rectangular, trapezoidal, or triangular. One of the earliest research projects conducted by Jonson and Illes [33] by analyzing data from more than 100 dam breach events concluded that the breach initially develops in a "V" shape with a ratio of 4:1 or 3:1 wide to deep. While according to De Almeida & Franco [34] the final breach shape is trapezoidal, this conclusion is based on collected historical dam failure records. They also conclude that, for the earth-fill dams, triangular shape for the breach might be assumed up to the time that the breach reaches the base of the embankments. Once the apex of the triangle reaches the basement of embankments, the breach propagates forming a trapezoidal shape expanding because of the lateral erosion. Another conclusion, from numerous field and laboratory experiments conducted within a European Union funded project implemented in 10 different countries, is that the breach side keeps vertical during the breach growth [35]. Unfortunately, records that describe the progress of the breach cross-section with time are still unavailable for actual dam break events. The main parameters that define the shape of a breach are shown in Figure 1, where, B_b is the breach bottom width (meter), B_{avg} is the average breach width (meter), h_b is the breach height (meter), h_w is maximum depth of water stored behind the breach (meter), W_{avg} is the average width of dam in direction of flow (meter), C is the width of the dam crest (meter), Z_d and Z_u are the slopes of the downstream and upstream faces of the embankment, respectively, and Z_b is the side slope of breach.

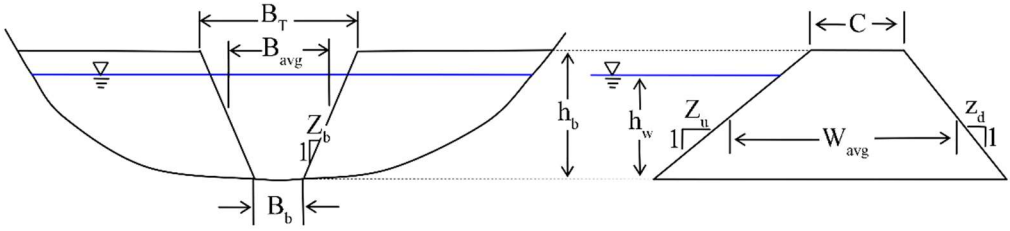

Figure 1 - Dam breach variable definition sketch. [36]

2.2. Breach Development

To understand the breach development, the progress of the breach in time and space should be investigated [37]. Breach initiation time is defined as the time starting from the first observable leak (e.g., overtopping, piping, and so forth) that launches warning, evacuation, or awareness, and ending when the breach formation phase started [38-39]. Within this stage phase (breach initiation), the flow amount is relatively small; and if the leak can be kept under control, the dam might not collapse. The phase of breach formation initiates at the moment when the dam failure is about to start and continues until when the breach reaches its maximum shape. The size of the dam reservoir plays a significant role. For a small capacity reservoir, the peak outflow from a dam breach may take place before the breach cross-section reaches its maximum shape, simply because of a rapid decline in reservoir water level during the breach progress. On the contrary, the peak outflow in the case of dams with a relatively large storage pool may occur when the breach fully develops. An initial assumption here is that a channel formed on the embankment body is often taken into consideration in all breach models. The initial channel determines the starting condition for the breaching progress. If no initial channel exists, then the succeeding phases of the breaching process will not happen. The fundamental characteristics of the breach channel define further breaching development. As the initial channel formation depends on many factors (e.g., flow characteristics, structure coverage, and improper/insufficient compaction), it is a difficult task to predict the exact initial location of the formed breach channel.

2.2.1. Hydraulics of Flow over the Dam

The breach flow hydrograph plays a significant role in the evaluation of the flood wave characteristics in the downstream regions. The flow through the breach channel can be simulated using either orifice equation (at the initial formation phase of piping failure), and the weir equation or the one-dimensional Navier-Stokes equation referred to as Saint–Venant equations.

The weir equation that estimates the discharge for the free flow (low tailwater) condition is expressed as:

$$Q = CLH^{3/2} \quad (1)$$

where, Q is the discharge, C ($m^{1/2}.s^{-1}$) is weir coefficient, L (m) is the weir crest length, and H (m) is energy head over the weir crest. In extreme cases, if tailwater arises up to the embankment crest, Eq. 1 becomes,

$$Q = C_s L H^{3/2} \quad (2)$$

where C_s is a coefficient for the submergence effect.

Attention should be given to the difference between the weir coefficient and the discharge coefficient. The weir coefficient is an aggregate parameter that includes the discharge coefficient, the gravitational constant, and constants based on geometric properties.

$$C = \frac{2}{3} C_d \sqrt{2g} \quad (3)$$

where C_d again is the dimensionless discharge coefficient [40-41].

Empirical Approaches to Dam-Break Analysis

A group of the most common experimental approaches for forecasting dam breach size and breach formation time were applied to evaluate breach parameters for a dam-break event. The employed approaches are MacDonald and Langridge-Monopolis [42], Bureau of Reclamation [36], Von Thun and Gillette [43], Froehlich [14]; and Xu and Zhang [44]. Furthermore, the type of failure, either overtopping or piping, was also examined in the study based on the parameters defined in Fig. 1. The empirical methods were formulated based on a statistical analysis of the data extracted from documented dam failures.

To estimate the width of the dam breach recommendations of Singh and Snorrason [45] was integrated. Their empirical formula was calculated in the approach based on twenty documented dam failure cases. The breach width is a function of only one variable, dam height, ranging between twice and five times of the height. Also, according to this study, they expressed that the dam failure time varied from a quarter-hour to one hour.

The study by MacDonald and Langridge-Monopolis [42], on the other hand, provides two sets of equations to accommodate the differences between the types of dams (e.g., earth-fill dam or other type dams). In their study, data set of fourty-two dam failure events were assessed to develop the regression equation that predicts the breach factors. Eqs. 4 and 5 that estimate the volume of eroded material (V_{er}, m^3) are functions of the volume of water that passes through the breach (V_{out}, m^3) and water depth (h_w, m) in the reservoir at the time of failure, for earth-fill dam type and other types, respectively. This study covered a range of dams with the height ranging between 4.27 m and 92.96 m and the available water volume between 0.0037 and 660.0 (10^6 m^3). For the time of failure, based on the calculated volume of material eroded, (t_f, hr) Eq. 6 was recommended.

$$V_{er} = 0.0261(V_{out} * h_w)^{0.769} \quad \text{(for earthfill dams)} \quad (4)$$

$$V_{er} = 0.00348(V_{out} * h_w)^{0.852} \quad \text{(for earth-fill dams with a clay core or rockfill dams)} \quad (5)$$

$$t_f = 0.0179(V_{er})^{0.364} \quad (6)$$

U.S. Department of the Interior, Bureau of Reclamation [36] provided a third approach to obtain the width of rectangular breach with respect to depth of the water in the upstream reservoir (Eq. 7). This formula can be used as a rule of thumb for choosing the ultimate breach width that can be used mostly in the hazard classification studies. This approach suggests that the time for breach to develop is around 1% of the breach width (Eq. 8).

$$B = 3\ h_w \tag{7}$$

$$t_f = 0.011\ \mathrm{B} \tag{8}$$

The fourth method put forward by Von Thun and Gillette [43] used the data obtained from fifty-seven historically recorded dam failure cases that were previously studied by both Froehlich [46] and MacDonald & Langridge-Monopolid [42] to recommend a relationship for predicting average breach width, B_{avg}. In the relationship, Eq. 9, B_{avg} is a function of reservoir water depth (h_w, m) and the coefficient (C_b, m). the data covered a range of where V_{out} (10^6 m^3) between 0.027 and 660 and height of dams (h_d, m) between 3.66 and 92.96. Besides, Von Thun and Gillette [43] stated that the majority of dams (89 %) have h_d less than 30 m and V_{out} less than 25 (10^6 m^3). The C_b values were directly related to the reservoir size and varied from 6.1 m for relatively small reservoirs to 54.9 m for large sized reservoirs.

$$B_{avg} = 2.5\ h_w + C_b \tag{9}$$

In addition to the developed relationship, it was also recommended to use 1H:1V breach slope side except for the dams with cohesive coresfor which a ratio of 1H:2V or even 1H:3V may be more suitable. Regarding to the breach formation time, the approach provides two set of equations based on the dam fill material Eqs. 10 through 13.

$$t_f = 0.02\ h_w + 0.25 \quad \text{(erosion resistive material)} \tag{10}$$

$$t_f = 0.015\ h_w \quad \text{(easily erodible)} \tag{11}$$

Breach development time as a function of (h_w and B_{avg}):

$$t_f = \frac{B_{avg}}{4h_w} \quad \text{(erosion resistive material)} \tag{12}$$

$$t_f = \frac{B_{avg}}{4h_w + 61.0} \quad \text{(highly erodible)} \tag{13}$$

The next approach investigated in the present study was originally developed by Froehlich [14] and exemplifies one of the most recent studies on dam breach. The study is seemingly an enhancement of one of his previous studies (Froehlich, 1987) covering a larger number of documented dam breach cases. The study states that in the case of overtopping type failure, the side slope ratio is 1H:1V, while for the piping or seepage failure the side slope ratio is 0.7H:1V.

Froehlich's suggested the following relationship (Eq. 14) for the average width of the breach (B_{avg}, m),

$$B_{avg} = 0.27\, K_0\, V_w^{0.32}\, h_b^{0.04} \tag{14}$$

where, K_o = 1.3 for overtopping, and K_o = 1.0 for other failure modes. The equation below considers that the breach formation time is directly proportional to reservoir volume (V_w, m^3) and inversely proportional to the breach height (h_b, m) (Eq. 15).

$$t_f = 63.2 \sqrt{\frac{V_w}{g\, h_b^2}} \tag{15}$$

In the last approach, considered in the present work, by Xu and Zhang [44], analyses were performed using a wide range of historically documented dam failure cases – 182 earth and rockfill dams from both U.S and China. However, due to data limitations their final formulas were developed using a relatively smaller subset (75 dams) of those dam break cases. The ranges of h_d and V_{out} used in the study are very similar to the ranges that were used by Von Thun and Gillette [43] (i.e., 3.2 m ≤ h_d ≤ 92 m; and 0.105 × 10^6 m^3 ≤ V_{out} ≤ 660 × 10^6 m^3). However, in this study most dams (around 80 %) have heights less than 30 m and V_{out} less than 25×10^6 m^3. They also, developed an equation (Eq. 16) to calculate the average breach width (B_{avg}, m).

$$\frac{B_{avg}}{h_b} = 0.787 \left(\frac{h_d}{h_r}\right)^{0.133} \left(\frac{V_w^{1/3}}{h_w}\right)^{0.652} e^{B_3} \tag{16}$$

where, h_r is 15 meters, which is the reference height used to distinguish between small and large dams, B_3 is the coefficient that depends on dam properties and equal to the summation of b_3, b_4, and b_5; b_3 is -0.226 for homogenous/zoned-fill, b_4 is equal to -0.389 and 0.149 for piping and overtopping, respectively, and b_5 represents the effect of erodibility of the dam (e.g., Ürkmez dam was considered to be medium erodible with b_5 = -0.14)

Unilke the previous methods, Xu & Zhang [44] method does not estimate the side slopes of the breach. Alternatively, the method calculates the top width of the breach (B_T, m) through Eq. 17 that governs the relationship between the breach top width and the height of the final breach.

$$\frac{B_T}{h_b} = 1.062 \left(\frac{h_d}{h_r}\right)^{0.092} \left(\frac{V_w^{1/3}}{h_w}\right)^{0.508} e^{(b_3+b_4+b_5)} \tag{17}$$

where b_3 is -0.089 for homogenous/zoned-fill, b_4 is equal to -0.239 and 0.299 for piping and overtopping, respectively; and b_5 is -0.062 for medium erodible dam.

All of the equations above help to estimate the breach geometry parameters suggested by the different approaches of earlier studies which then serve as input for hydraulic modelling.

3. METHODS

In the presented study, five of the most popular experimental approaches for predicting dam breach characteristics (e.g., dam breach size and breach formation time) were employed to estimate breach parameters for the Ürkmez Dam. The study site of Ürkmez Dam was selected as it is in a touristic region with the residential area right on the dam downstream (Fig. 2). It is located 3 km north of Ürkmez township in the province of İzmir in Turkey. The dam was built to supply drinking water and provide irrigation. The General Directorate for State Hydraulic Works (DSI) completed the construction in 1990 and the dam started with the irrigation function. In 2004, a municipal water treatment plant was built and started functioning.

The breach modelling techniques were formulated from the statistical analysis of data derived from the recorded dam failures of a wide range of dam sizes. These approaches were used to estimate Ürkmez Dam breach characteristics subjected to numerous scenarios of failure mode type (e.g., overtopping and piping) with varying ranges of initial upstream reservoir water levels. A decreasing interval of 2 m - from the maximum upstream reservoir storage level (48 m a.s.l.), were studied for these methods. The centerline of the dam was assumed to be the dam breach location for both piping and overtopping failure types. As the weir and piping coefficients for the earthen sand and gravel type of dams (similar to the Ürkmez Dam case) are recommended to be between 2.6 and 3.0 in case of overtopping mode, and 0.5 to 0.6 in piping failure mode [1], these coefficients were set to be as 2.8 and 0.55, for overtopping and piping failure modes, respectively. In the case of piping failure mode, the breach start level though piping was considered to be at the level equal to the half of the water height in the reservoir ($h_w/2$).

Figure 2 - Ürkmez Dam Location Map

The Probable Maximum Precipitation (PMP) was calculated using [47] statistical method based on the annual maximum precipitation observations for 67 years in the period 1938-2015. The Probable Maximum Flood (PMF) hydrograph generated from the PMP was used as input hydrograph feeding the HEC-RAS 5.0.7 hydraulic model. Since the topography of upstream reservoir was modeled accurately, the level pool routing method was used conveniently. The study area was modelled using inline structure to present the dam body, a storage area to model the upstream reservoir and a continuous 2-dimensional mesh with 20-meter resolution to model the downstream area, while a 1-meter mesh resolution was used in representing the river and spillway centerlines. The main riverbed was assumed to be the breach final bottom elevation. The Saint-Venant full-momentum set of equations were used to determine the flood hydrograph produced by a dam breach for each scenario setting.

4. RESULTS AND DISCUSSION

4.1. Maximum Discharge and Time of its Occurrence

The resulting flood hydrograph associated with dam-break in the case of Ürkmez Dam was calculated by using the Saint-Venant full momentum set of equations in HEC-RAS 5.0.7 with a different initial reservoir level for five different empirical approaches for both overtopping and piping failure modes as shown in Table 1. The flood hydrographs were

Table 1 - Maximum discharge & Time to peak discharge for all scenarios

Approach	Variable	Unit	Failure Type	Initial Reservoir Level (m)				
				48.0	**46.0**	**44.0**	**42.0**	**40.0**
USBR	Q_p	(10^3 m^3/s)	Over top.	5.85	5.89	5.91	5.92	5.93
	T_p	min.		23.05	22.92	22.88	22.90	22.95
	Q_p	(10^3 m^3/s)	Piping	4.87	4.92	4.95	4.97	4.98
	T_p	min.		25.05	24.82	24.93	27.88	25.02
Von Thun & Gillette Eq. (10)	Q_p	(10^3 m^3/s)	Overtopping	7.64	7.69	7.71	7.72	7.72
	T_p	(min.)		16.05	15.83	15.88	15.92	16.02
Eq. (12)	Q_p	(10^3 m^3/s)		7.37	7.41	7.44	7.44	7.45
	T_p	(min.)		18.00	17.87	17.88	17.93	17.59
MacDonald & Monopolis	Q_p	(10^3 m^3/s)	Over top.	2.90	2.98	3.00	3.02	3.03
	T_p	min.		64.00	64.82	64.88	63.90	63.95
	Q_p	(10^3 m^3/s)	Piping	2.73	2.78	2.81	2.85	2.85
	T_p	min.		64.02	61.82	61.88	61.90	61.98
Xu & Zhang	Q_p	(10^3 m^3/s)	Over top.	3.75	3.82	3.87	3.89	3.91
	T_p	min.		56.12	55.83	54.88	55.90	54.97
	Q_p	(10^3 m^3/s)	Piping	2.88	2.94	2.98	3.00	3.02
	T_p	min.		65.08	64.83	64.88	64.93	64.95

obtained at a point immediately after the downstream face of the dam. Here, slight increases are observed in the outflow hydrograph peak quantities in a pattern inversely proportional with the initial reservoir levels. The rationale behind this is that the dam becomes subject to different rates of inflow (observed from the PMF hydrograph) as the time passes from the initial reservoir water elevation. Indeed, higher rates of flow will have been accessed at the breach formation time in the case of lower initial reservoir elevations so that longer time will be required to allow the breach process to initiate (also considering the additional time for the full development of breach geometry on top of the breach start through the gradual development of breach geometry). As shown in Figs. 3a and 3b, the overtopping failure type has also a tendency to provide higher peak discharge value than the piping failure type. It was observed also that, Von Thun & Gillette approach (Eq. 12), which estimates the breach development time as a function of h_w and B_{avg}, provides time to peak longer than the one obtained by Eq. 10 (i.e., time to peak as function of h_w). Besides, the peak discharge obtained using (t_f) from Eq. 12 is always less than the peak quantity obtained through using (t_f) from Eq. 10.

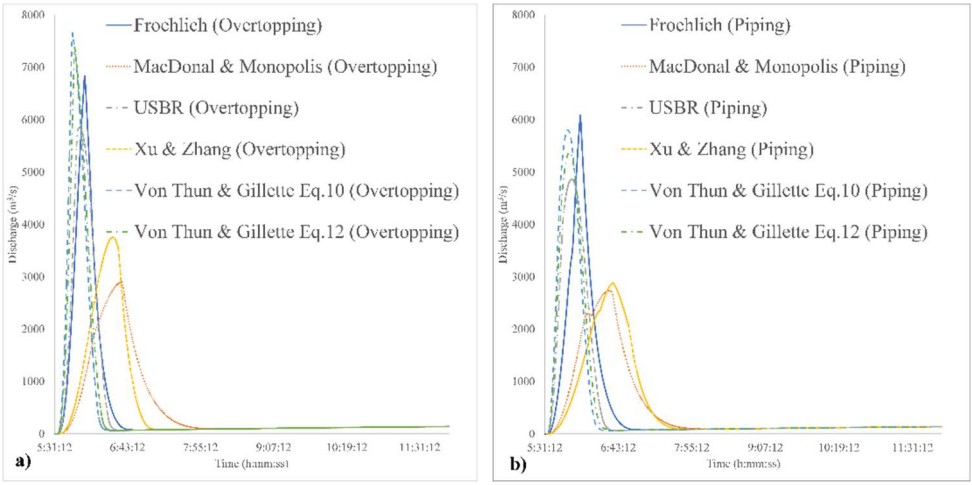

Figure 3 - a) Flood hydrographs when reservoir elevation is at 48 m a.s.l. for all approaches for Overtopping failure mode, b) Flood hydrographs when reservoir elevation is at 48 m a.s.l. for all approaches for piping failure mode

4.2. Failure Mode Impact on Flood Hydrographs

With the aim of examining the effect of failure type on the resulting hydrograph. Firstly, the geometry of the breach for all the approaches were predicted for the maximum reservoir level for both overtopping and piping failure mode (Figs. 3a, 3b). Figs. 3a, and 3b clearly reveal that, for the same reservoir level (i.e.,48 m), there are two differentiated sets of hydrograph patterns that are associated with the different methods applied. The first set of hydrographs has the highest amplitudes with higher discharge peaks that resulted in less times to peaks as well as the lower base times. The hydrographs of this first pattern were calculated by using

Von Thun & Gillette, USBR, and Froehlich approaches. Xu & Zhang and MacDonald & Monopolis prediction approaches established the second set of hydrographs which are characterized by relatively longer times to peak discharges (and longer base times) and approximately halved peak values with respect to the former group values. This pattern remains the same for both overtopping and piping failure types. Besides, while Xu & Zhang approach provides a higher peak value (e.g., +22.5 %) in the overtopping failure mode than MacDonald & Monopolis method, its peak attenuates to become nearly at the same level with MacDonald & Monopolis method for the piping mode. Secondly, the effect of failure mode was also investigated by varying the initial water level for the upstream reservoir (e.g., 40 m, 42 m, 44 m, 46 m, and 48 m).

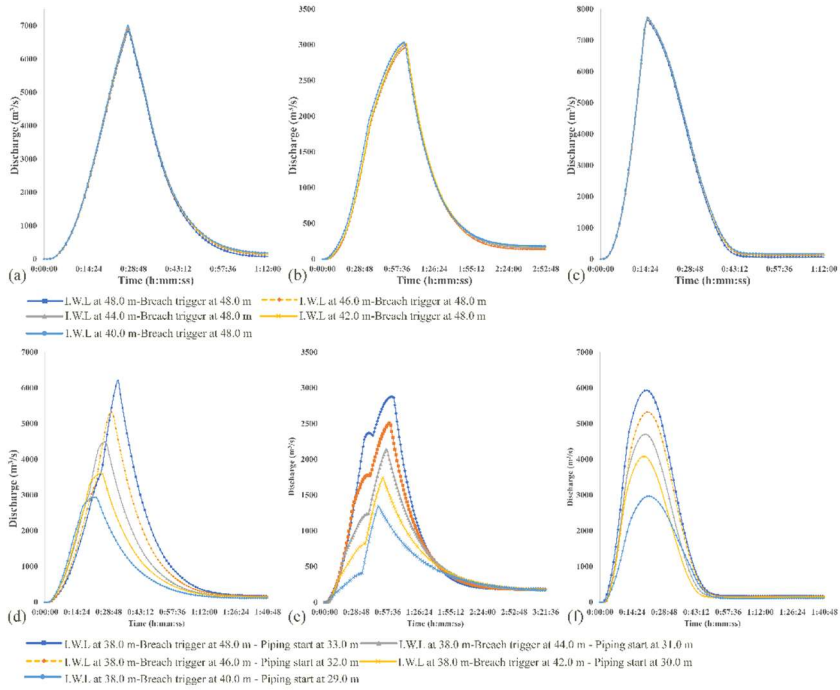

Figure 4 - Flood hydrographs for different initial water levels (I.W.L) using (a) Froehlich approach, (b) MacDonald & Monopolis approach, (c) Von Thun & Gillette (Eq. 10) approach for overtopping failure modes, and (d) Froehlich approach, (e) MacDonald & Monopolis approach, and (f) Von Thun & Gillette (Eq. 10) approach for piping failure modes.

Figs. 4a to 4c show that a very minimal change was observed when varying the initial water level for the overtopping failure mode, where, the breach trigger at elevation 48.0 m. Figs. 4d to 4f illustrate the flood hydrographs that were generated using piping failure modes (for piping to start at the half of the water height in the reservoir above the reservoir bottom elevation (Z_b) of 18 m; i.e., $Z_b + h_w/2$) against the initial water level (I.W.L) assumption of 38 m. (e.g., the piping breach elevation of 33.0 m is computed for the breach trigger

consideration at the reservoir water level of 48.0 m that corresponds to 30.0 m reservoir water depth (h_w) above Z_b). It is also apparent from the graphs of the piping mode that the time to peak evolved gradually for the Frohlich hydrographs for varying initial water levels associated with corresponding piping start levels, while in the latter two, the changing input variables for inducing the piping did not make significant effect on the peak arrival time.

4.3. Sensitivity Analysis

With the aim to investigate which parameter of dam breach has more influence on the result, a sensitivity analysis was applied by using the Froehlich (2008) [14] approach with the overtopping failure type and dam maximum operating water elevation at 48 m a.s.l. To determine the controlling parameter, the breach formation time (t_f), the average breach width (B_{avg}), and side slope (Z_b) were increased by 25 %, 50 %, 75 % and 100 % and then reduced by 25 %, 50 % and 75 %, respectively. The resulting flood hydrographs directly at the downstream side of the dam were estimated for each individual case. The sensitivity analysis for B_{avg} clearly shows that an increase of breach width by a constant percentage tends to increase the maximum discharge value and at the same time decrease T_p and vice versa. As Figs. 5a and 5b reveal, doubling the value of B_{avg} leads to an increase in the maximum discharge value by 34 % while dropping the time to peak up to 50 %.

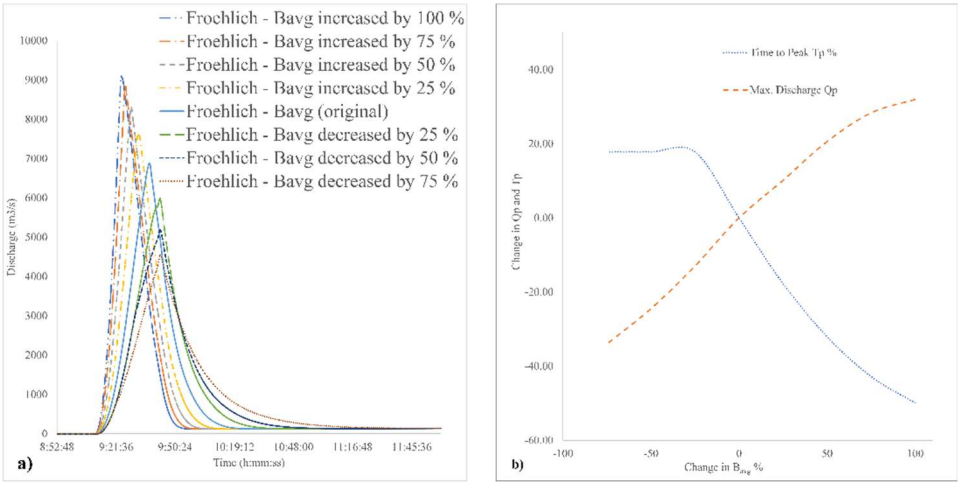

Figure 5 - a) Flood hydrographs for different B_{avg} values at dam site, and b) percent change in Q_p and T_p with B_{avg}

Apparently, no remarkable variation was distinguished in time to peak and a minor difference in peak discharge value with respect to the corresponding changes in breach side slopes. Although, adjusting the breach side slope leads to a change in breach cross-section area, decreasing the breach side slope by 75 % led to change by 0.0 % and -15 % in time to peak and peak discharge, respectively. Therefore, the breach side slope effect in the case of Ürkmez dam can be considered negligible, as Figs. 6a and 6b indicate.

The results obtained by varying the time of breach formation - with standardization of all other parameters (e.g., average breach width (B_{avg}) and side slope (Z_b) of the breach cross-section) - suggest that maximum discharge value, Q_p and the time of peak discharge, T_p are significantly sensitive to the change in time for the breach to fully develop. As Table 2, Figs. 7a and 7b suggest, increasing the breach formation time by 50 %, from 0.55 hr to 0.83 hr, led to a decrease in Q_p by 23.18 % and an increase in T_p by 46.44 %. Nevertheless, declining breach formation time by 50 %, from 0.55 hr to 0.14 hr, led to an increase in Q_p by 32 % while T_p was halved.

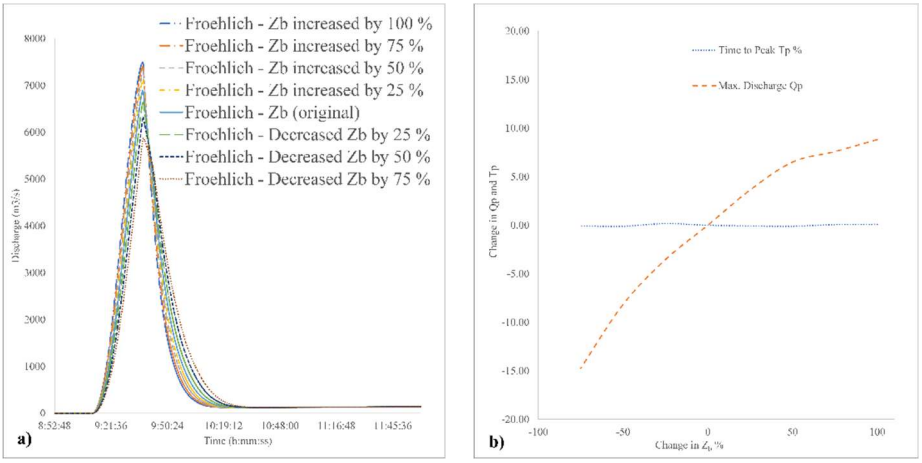

Figure 6 - a) Flood hydrographs for different Z_b values at the dam site, and b) percent change in Q_p and T_p against varying Z_b.

Table 2 - The maximum discharge and time to the maximum values against varying breach formation times

t_f (hr)	t_f dif. (%)	Q_p (10^3 m^3/s)	Q_p dif. (%)	T_p (min)	T_p dif (%)	Note
1.10	t_f +100%	4.17	-39.33	53.07	88.86	
0.96	t_f +75%	4.66	-32.24	47.15	67.79	**Increased t_f**
0.83	t_f +50%	5.29	-23.18	41.15	46.44	
0.69	t_f +25%	6.04	-12.25	35.08	24.84	
0.55	t_f +0%	6.88	0.00	28.10	0.00	**Original t_f**
0.41	t_f -25%	7.87	14.32	21.13	-24.80	
0.28	t_f -50%	9.08	31.97	14.08	-49.89	**Decreased t_f**
0.14	t_f -75%	10.77	56.57	8.07	-71.28	

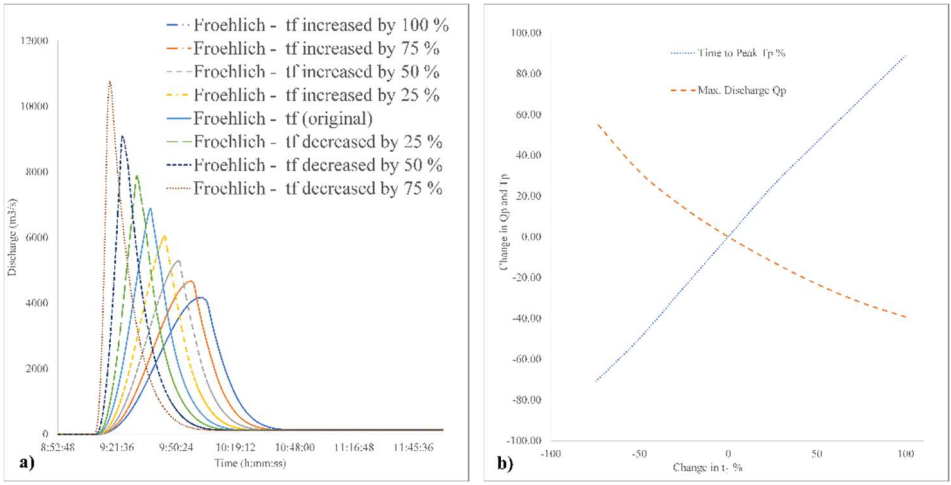

Figure 7 - a) Flood hydrographs for different t_f at the dam site, and b) percent change in Q_p and T_p with respect to t_f.

The results from the sensitivity analysis in the current study help reveal that the breach side slope has no significant impact on neither the peak discharge arrival time nor the peak discharge value itself. Nevertheless, the outflow hydrograph is remarkably sensitive to the breach width and is extremely sensitive to the breach formation time. These findings that resulted from the disconnected study on a site with varied dam characteristics and topography features as such proved to be in a reconfirmed agreement with the previous studies on the same subject in support of the sensitivity aspects of the breach parameters (e.g., [6], [38], [48-50]).

4.4. Flood Inundation and Hazard Mapping

The main objective of flood hazard mapping is to identify areas under the risk of flooding, and thus to contribute to both flood risk management and the post-disaster recovery planning. Dam break connected flood hazard maps typically unveil the expected flood extent, depth, and velocity characteristics in the downstream. In the case of dam break flood mapping, flood hazard can vary significantly across both the temporal and spatial scales, particularly with a combined impact of flood velocity and depth.

U.S. Bureau of Reclamation (1988) provides guidance (Downstream Hazard Classification Guideline [36] to evaluate the fluctuating degrees of flood hazard that occurs across a floodplain. For the scope of this study, a classification for possible hazard for adults, considered to be over 150 cm tall and weighing over 54 kg [36], is mainly carried out based on the flood danger relationship with depth and velocity. The classification scheme produces three hazard levels (through high-danger zone, judgment/transition zone, and low-danger zone definitions). In the context of the presented study, a comparison between the hazard inundation mapping produced by using the Froehlich [14] (Fig. 8) and MacDonald & Monopolis [42] methods (Fig. 9) both for overtopping breach types were provided since these

literature sources yielded notably dissimilar results for both the time to peak and the peak discharge quantities as clearly shown in Fig. 3a. Figs. 8 and 9 show the temporal series of flood hazard mapping that covered an area of 5 km^2 downstream of the dam. It is worth to note here that the resulting hazard zones associate with the probable maximum event that may be experienced in the case study, though there may be other studies that deal with the flood issue in different aspects. Differing from the main objective of sensitivity analysis, some relate to the modeling and validation of an actual flood event experience (e.g., [10], [15], [24]) while some others more consider scenario analyses (e.g., [19]).

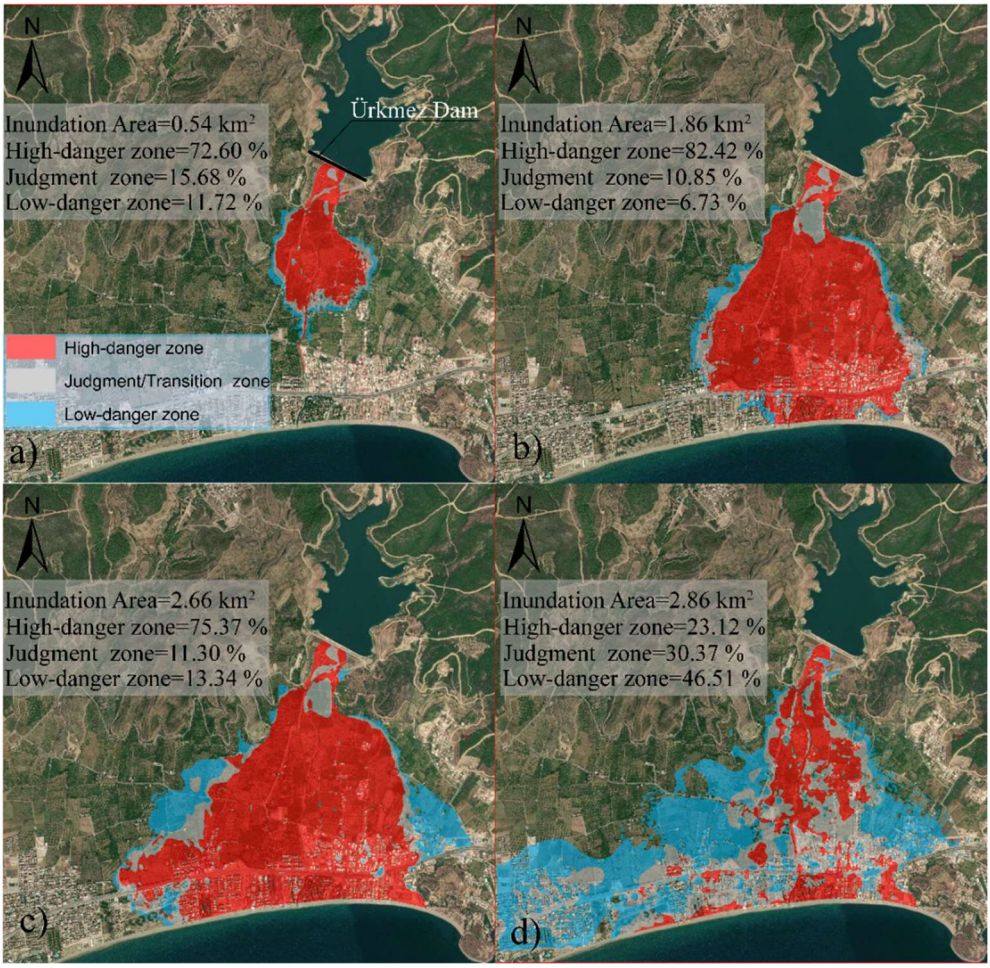

Figure 8 - The Spatio-temporal change in water extent and hazard classification using Froehlich [14] method after a) 15 min, b) 25 min, c) 35 min, d) 60 min.

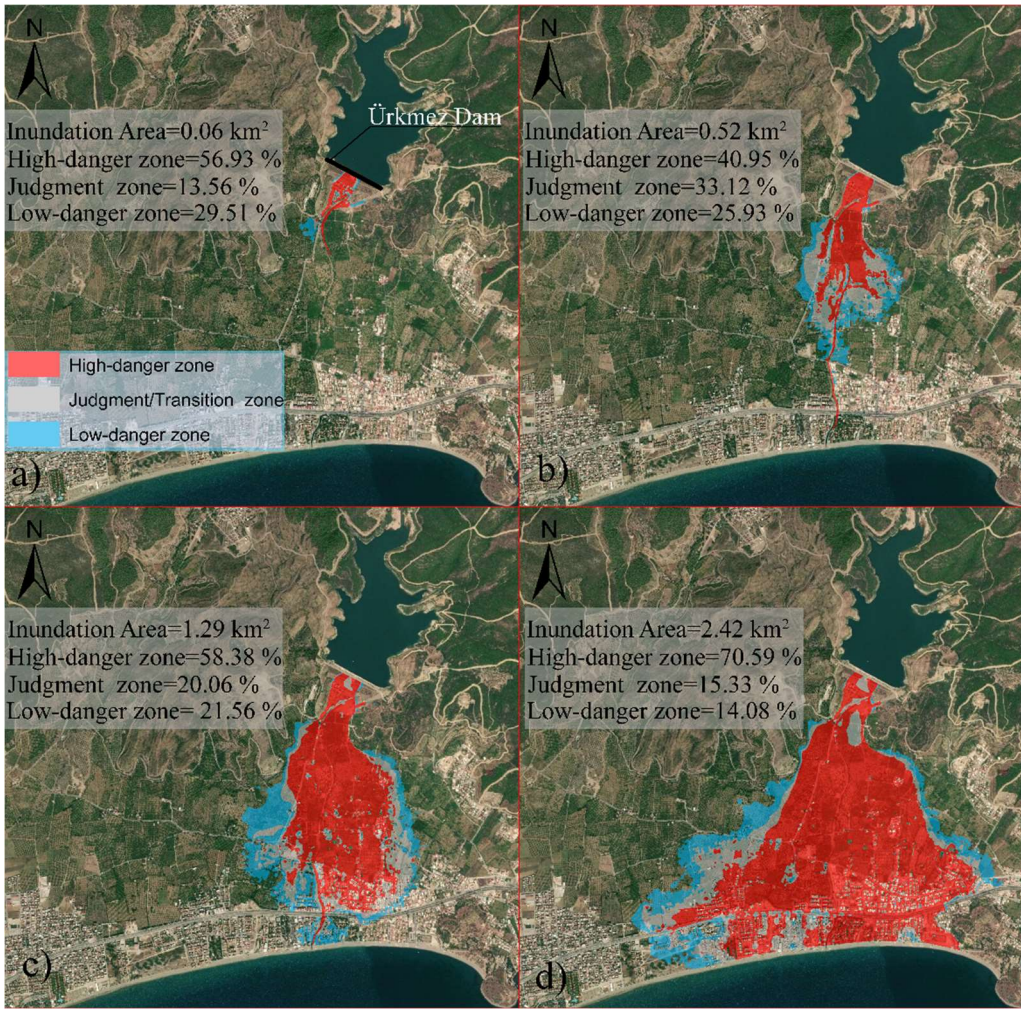

Figure 9 - The Spatio-temporal change in water extent and hazard classification using MacDonald & Monopolis [51] method after a) 15 min, b) 25 min, c) 35 min, d) 60 min.

5. CONCLUSIONS

This study explored the consequences of a hypothetical dam failure in the case of an embankment dam with a built-up downstream area of 5 km^2. The HEC-RAS two-dimensional hydrodynamic model was used to simulate dam failure and propagation of the flood wave for extensive set of scenarios (96 in total varying with respect to initial conditions and breach formation characteristics). Scenarios were practiced testing the varying impacts of overtopping and piping failure modes. Besides, 5 initial reservoir levels (e.g., 48 m, 46 m, 44 m, 42 m and 40 m a.s.l) were studied in each approach. A very sensitive DTM was developed as well as the worst-case scenario was studied by considering the PMF hydrograph as input

for the hydraulic model. The differences in the hydraulic model predictions caused by alternating the initial conditions were analyzed. A sensitivity analysis on the breaching parameters was mainly performed. The study investigated flooding impacts based on the flood hydrographs resulting from dam break phenomenon. A series of breach prediction methods that commonly appeared in relevant scientific literature were employed in the case study.

Based on comparisons with an observational judgment among all the methods employed in the study, the USBR and Von Thun & Gillette approaches estimated the highest peaks and the lowest times to corresponding peaks, Froehlich (2008) method provided moderate outputs for the both quantities (peak discharge and peak time) while the lowest peaks against delayed peak arrival times were estimated through the MacDonald & Langridge-Monopolis and Xu & Zhang equations. In general, the piping failure modes that were simulated in all empirical approaches tend to give lower peak flood discharges in comparison to the overtopping failure mode as expected.

The sensitivity analysis points out that both the peak discharge and the peak arrival time (i.e., time to peak) show great sensitivity to the breach full development time (t_f) parameter (even following an almost identity line relationship with T_p) and again a considerable sensitivity to the breach width (B_{avg}) parameter. Besides, the results provided strong indication to infer that the breach side slope (Z_b) does not affect the time to peak discharge at all, even though its negligible impact on the evolution of the peak discharge may still be observed.

Concerning the targeted study area, the obtained results show that the case study area, Ürkmez reservoir, represents a significant threat to downstream areas in a probable event of dam break; as indicated by the hazard maps; greater portion of the inundated area is subject to high-danger hazard level in around 30 mins after the break event.

The obtained results provide decision makers, urban & emergency planners, and vulnerable communities in the end, to help formulate evacuation procedures and to consider an adapted site planning in the areas especially associated with high and intermediate (transition) hazard levels. The presented work is targeted to provide a contribution to the field of dam break studies in its tailored context with the use of method-specific breach parameter estimations instead of user defined assignments (i.e., through the suggestions of the methods themselves) when investigating the sensitivity of the parameters governing the outflow discharge characteristics.

References

[1] G. Brunner, Using HEC-RAS for Dam Break Studies, TD-39, 2014.

[2] M. Zagonjolli, Dam break modelling, risk assessment and uncertainty analysis for flood mitigation, Delft University of Technology & UNESCO-IHE Institute for Water Education, 2007.

[3] C. A. Pugh and D. W. Harris, Prediction of landslide-generated water waves, 1982.

[4] L. Li, M. Cargnelutti, and C. Mosca, Dam-break events,flood damage, Piemonte region, Italy, Water Resour. Manag., vol. 5, pp. 261–270, 1991.

[5] Z. Bozkuş and A. Kasap, Comparison of physical and numerical dam-break simulations, Turkish J. Eng. Environ. Sci., vol. 22, no. 5, pp. 429–443, 1998.

[6] Z. Bozkuş and A. I. Güner, Pre-event dam failure analyses for emergency management, Turkish J. Eng. Environ. Sci., vol. 25, no. 6, pp. 627–641, 2001.

[7] P. Brufau, M. E. Vázquez-Cendón, and P. García-Navarro, A numerical model for the flooding and drying of irregular domains, Int. J. Numer. Methods Fluids, vol. 39, no. 3, pp. 247–275, May 2002, doi: 10.1002/fld.285.

[8] A. M. Yanmaz and M. R. Beşer, On the reliability-based safety analysis of the Porsuk Dam, Turkish J. Eng. Environ. Sci., vol. 29, no. 5, pp. 309–320, 2005, doi: 10.3906/sag-1203-6.

[9] J. A. Vásquez and J. G. A. B. Leal, Two-dimensional dam-break simulation over movable beds with an unstructured mesh, Proc. Int. Conf. Fluv. Hydraul. - River Flow 2006, vol. 2, pp. 1483–1491, 2006, doi: 10.1201/9781439833865.ch158.

[10] F. Alcrudo and J. Mulet, Description of the Tous Dam break case study (Spain), J. Hydraul. Res., vol. 45, no. sup1, pp. 45–57, Dec. 2007, doi: 10.1080/00221686.2007.9521832.

[11] A. Palumbo, S. Frazão, L. Goutiere, D. Pianese, and Y. Zech, Dam-break flow on mobile bed in a channel with a sudden enlargement, in Proceedings international conference on Fluvial Hydraulics, 2008, pp. 645–654.

[12] F. Macchione, Model for Predicting Floods due to Earthen Dam Breaching. I: Formulation and Evaluation, J. Hydraul. Eng., vol. 134, no. 12, pp. 1688–1696, Dec. 2008, doi: 10.1061/(ASCE)0733-9429(2008)134:12(1688).

[13] F. Macchione and A. Rino, Model for Predicting Floods due to Earthen Dam Breaching. II: Comparison with Other Methods and Predictive Use, J. Hydraul. Eng., vol. 134, no. 12, pp. 1697–1707, Dec. 2008, doi: 10.1061/(ASCE)0733-9429(2008)134:12(1697).

[14] D. C. Froehlich, Embankment Dam Breach Parameters and Their Uncertainties, Environ. Prot., vol. 134, no. May 2011, pp. 1708–1721, Dec. 2008, doi: 10.1061/(ASCE)0733-9429(2008)134:12(1708).

[15] S. E. Yochum, L. A. Goertz, and P. H. Jones, Case Study of the Big Bay Dam Failure: Accuracy and Comparison of Breach Predictions, J. Hydraul. Eng., vol. 134, no. 9, pp. 1285–1293, 2008, doi: doi:10.1061/(ASCE)0733-9429(2008)134:9(1285).

[16] X. Ying, J. Jorgeson, and S. S. Y. Wang, Modeling Dam-Break Flows Using Finite Volume Method on Unstructured Grid, Eng. Appl. Comput. Fluid Mech., vol. 3, no. 2, pp. 184–194, 2009, doi: 10.1080/19942060.2009.11015264.

[17] J. Singh, M. S. Altinakar, and Y. Ding, Two-dimensional numerical modeling of dam-break flows over natural terrain using a central explicit scheme, Adv. Water Resour., vol. 34, no. 10, pp. 1366–1375, 2011, doi: https://doi.org/10.1016/j.advwatres.2011.07.007.

[18] P. Marco, M. Andrea, T. Massimo, and V. Giulia, 1923 Gleno Dam Break: Case Study and Numerical Modeling, J. Hydraul. Eng., vol. 137, no. 4, pp. 480–492, Apr. 2011, doi: 10.1061/(ASCE)HY.1943-7900.0000327.

[19] Z. Bozkuş and F. Bağ, Virtual Failure Analysis of the Çınarcık Dam, Tek. Dergi/Technical J. Turkish Chamb. Civ. Eng., vol. 22, no. 4, pp. 5675–5688, 2011.

[20] Q. Honghai, S. M. Altinakar, H. Qi, and M. S. Altinakar, GIS-Based Decision Support System for Dam Break Flood Management under Uncertainty with Two-Dimensional Numerical Simulations, J. Water Resour. Plan. Manag., vol. 138, no. 4, pp. 334–341, Jul. 2012, doi: doi:10.1061/(ASCE)WR.1943-5452.0000192.

[21] H. Mahdizadeh, S. K. Peter, and R. D. Benedict, Flood Wave Modeling Based on a Two-Dimensional Modified Wave Propagation Algorithm Coupled to a Full-Pipe Network Solver, J. Hydraul. Eng., vol. 138, no. 3, pp. 247–259, Mar. 2012, doi: 10.1061/(ASCE)HY.1943-7900.0000515.

[22] S. Bosa and M. Petti, A Numerical Model of the Wave that Overtopped the Vajont Dam in 1963, Water Resour. Manag., vol. 27, no. 6, pp. 1763–1779, 2013, doi: 10.1007/s11269-012-0162-6.

[23] G. Tsakiris and M. Spiliotis, Dam- Breach Hydrograph Modelling: An Innovative Semi- Analytical Approach, Water Resour. Manag., vol. 27, no. 6, pp. 1751–1762, 2013, doi: 10.1007/s11269-012-0046-9.

[24] T. Moramarco, S. Barbetta, C. Pandolfo, A. Tarpanelli, N. Berni, and R. Morbidelli, Spillway Collapse of the Montedoglio Dam on the Tiber River, Central Italy: Data Collection and Event Analysis, J. Hydrol. Eng., vol. 19, no. 6, pp. 1264–1270, Jun. 2014, doi: 10.1061/(ASCE)HE.1943-5584.0000890.

[25] A. S. Chen, B. Evans, S. Djordjević, and D. A. Savić, A coarse-grid approach to representing building blockage effects in 2D urban flood modelling, J. Hydrol., vol. 426–427, pp. 1–16, 2012, doi: 10.1016/j.jhydrol.2012.01.007.

[26] A. S. Chen, B. Evans, S. Djordjević, and D. A. Savić, Multi-layered coarse grid modelling in 2D urban flood simulations, J. Hydrol., vol. 470–471, pp. 1–11, 2012, doi: 10.1016/j.jhydrol.2012.06.022.

[27] V. Bellos and G. Tsakiris, Comparing Various Methods of Building Representation for 2D Flood Modelling In Built-Up Areas, Water Resour. Manag., vol. 29, no. 2, pp. 379–397, 2015, doi: 10.1007/s11269-014-0702-3.

[28] Ş. Elçi, G. Tayfur, İ. Haltas, and B. Kocaman, Baraj Yıkılması Sonrası İki Boyutlu Taşkın Yayılımının Yerleşim Bölgeleri İçin Modellenmesi, Tek. Dergi/Technical J. Turkish Chamb. Civ. Eng., vol. 28, no. 3, pp. 7955–7975, Jul. 2017, doi: 10.18400/tekderg.307456.

[29] İ. Haltas, S. Elçi, and G. Tayfur, Numerical Simulation of Flood Wave Propagation in Two-Dimensions in Densely Populated Urban Areas due to Dam Break, Water Resour. Manag., vol. 30, no. 15, pp. 5699–5721, Dec. 2016, doi: 10.1007/s11269-016-1344-4.

[30] M. Ş. Güney, G. Tayfur, G. Bombar, and S. Elci, Distorted Physical Model to Study Sudden Partial Dam Break Flows in an Urban Area, J. Hydraul. Eng., vol. 140, no. 11, p. 5014006, 2014, doi: doi:10.1061/(ASCE)HY.1943-7900.0000926.

[31] I. Haltas, G. Tayfur, and S. Elci, Two-dimensional numerical modeling of flood wave propagation in an urban area due to Ürkmez dam-break, İzmir, Turkey, Nat. Hazards, vol. 81, no. 3, pp. 2103–2119, 2016, doi: 10.1007/s11069-016-2175-6.

[32] S. Oguzhan and A. Ozgenc Aksoy, Experimental investigation of the effect of vegetation on dam break flood waves, J. Hydrol. Hydromechanics, no. 2016, pp. 231–241, 2020, doi: 10.2478/johh-2020-0026.

[33] F. Jonson and P. Illes, A Classification of Dam Failures, Water Power Dam Constr., vol. 28, no. 12, pp. 43–45, 1976.

[34] A. B. De Almeida and A. B. Franco, Modeling of Dam-Break Flow BT - Computer Modeling of Free-Surface and Pressurized Flows, M. H. Chaudhry and L. W. Mays, Eds. Dordrecht: Springer Netherlands, 1994, pp. 343–373.

[35] M. Morris, Final Technical Report – January 2005, 2005.

[36] USBR, Downstream Hazard Classification Guidelines, Bureau of Reclamation, United States Department of the Interior, 1988, Denver, Colorado, 1988.

[37] K. A. Vaskinn et al., Physical Modeling of Breach Formation - Large scale field tests, in Proceedings of Dam Safety, 2004, pp. 1–16.

[38] T. L. Wahl, Prediction of Embankment Dam Breach Parameters - A Literature Review and Needs Assesment, 1998. doi: DSO-98-004.

[39] S. Dhiman and K. C. Patra, Experimental study of embankment breach based on its soil properties, ISH J. Hydraul. Eng., no. December, pp. 1–11, 2018, doi: 10.1080/09715010.2018.1474500.

[40] R. P. George, C. R. David, P. Miller, H. G. Yung, E. C. Paul, and M. Temple, Mechanics of Overflow Erosion on Embankments. II: Hydraulic and Design Considerations, J. Hydraul. Eng., vol. 115, no. 8, pp. 1056–1075, Aug. 1989, doi: 10.1061/(ASCE)0733-9429(1989)115:8(1056).

[41] C. Goodell, Weir Equations in HEC-RAS, The RAS Solution - The Place for HEC-RAS Modellers, 2016. https://www.kleinschmidtgroup.com/ras-post/weir-equations-in-hec-ras/ (accessed Jul. 16, 2020).

[42] C. T. MacDonald and J. Langridge-Monopolis, Breaching Charateristics of Dam Failures, J. Hydraul. Eng., vol. 110, no. 5, pp. 567–586, May 1984, doi: 10.1061/(ASCE)0733-9429(1984)110:5(567).

[43] J. L. Von Thun and D. R. Gillette, Guidance on breach parameters. Denver, Colorado: U.S. Dept. of the Interior, Bureau of Reclamation, 1990.

[44] Y. Xu and L. M. Zhang, Breaching Parameters for Earth and Rockfill Dams, J. Geotech. Geoenvironmental Eng., vol. 135, no. 12, pp. 1957–1970, Dec. 2009, doi: 10.1061/(ASCE)GT.1943-5606.0000162.

[45] K. P. Singh and A. Snorrason, Sensitivity of outflow peaks and flood stages to the selection of dam breach parameters and simulation models, Journal of Hydrology, vol. 68, no. 1–4. pp. 295–310, 1984, doi: 10.1016/0022-1694(84)90217-8.

[46] D. C. Froehlich, Embankment-Dam Breach Parameters, in Hydraulic Engineering, Proceedings of the 1987 National Conference., 1987, pp. 570–575, [Online]. Available: http://pubs.er.usgs.gov/publication/70014497.

[47] D. M. Hershfield, Method for Estimating Probable Maximum Rainfall, J. Am. Water Works Assoc., vol. 57, no. 8, pp. 965–972, 1965, doi: 10.1002/j.1551-8833.1965.tb01486.x.

[48] A. W. Petrascheck and P. A. Sydler, Routing of dam break floods, Int. Water Power Dam Constr., vol. 36, no. 7, 1984.

[49] Z. Bozkuş, Dam Break Analyses for Disaster Management (in Turkish), Tek. Dergi, vol. 15, no. 74, pp. 3335–3350, 2004.

[50] T. A. Basheer, A. Wayayok, B. Yusuf, M. D. R. Kamal, and M. Rowshon, Dam breach parameters and their influence on flood hydrographs for Mosul dam, J. Eng. Sci. Technol., vol. 12, no. 11, pp. 2896–2908, 2017.

[51] T. C. MacDonald and J. Langridge-Monopolis, Breaching Charateristics of Dam Failures, J. Hydraul. Eng., vol. 110, no. 5, pp. 567–586, May 1984, doi: 10.1061/(ASCE)0733-9429(1984)110:5(567).